Resonance Scattering of Slow Electrons from H_2 and CO Angular Distributions

H. Ehrhardt, L. Langhans, F. Linder, and H. S. Taylor*,†
Physikalisches Institut der Universität Freiburg, Freiburg, Germany
(Received 10 April 1968)

Energy and angular dependences of the elastic and inelastic scattering of electrons from H_2 and CO have been measured in the energy range from 0.5 eV to 10 eV and for scattering angles ranging from 5 to 110°. The elastic cross sections are composed of potential and resonance scattering and therefore are difficult to interpret. The excitation of molecular vibrations, i.e., scattering into inelastic channels, contains predominant contributions from short-lived negative ion compound states. The qualitative agreement of the measured angular dependence with that predicted from pure resonant scattering considerations is shown to be able to fix certain symmetry quantum numbers of the molecular state. Moreover, characteristic and similar σ-, π-, Δ-... type angular dependences throughout the whole energy range of the molecular resonance (independent of the final vibrational state) are presented as a means of verifying the presence of a resonance, even when the short lifetime masks the usually characteristic resonant peaks. The half-width of the $CO^-\,^2\pi$ state is about 0.4 eV, that for $H_2^-\,^2\Sigma_u^+$ between 2 and 4 eV. Absolute total cross sections for the different inelastic channels are given. The resonances of N_2, CO, and H_2 are compared with the predictions of the single-particle-shape resonance model and their physical properties are discussed using the different potential energy terms at large distances between the additional electron and the molecule. Throughout, stress is laid on the importance of choosing the proper experiment (i.e., exit channel) when one wishes to study a resonance. Predictably, in using angular dependence, certain channels hide and others exhibit the presence of the resonance.

The existence of short-lived negative ion states, formed in the scattering of low-energy electrons with molecules, has been established in several papers experimentally as well as theoretically. For this purpose measurements have been made of the: i, energy dependence of the attenuation of an electron beam after passing through a gas-filled scattering chamber,[1-3] ii, the energy dependence of the elastic and inelastic scattering cross section in the forward direction or into different scattering angles,[4-8] and iii, the energy dependence of the total cross section for the dissociative attachment process.[9,10] In certain energy ranges resonances are seen (methods i and ii), i.e., considerable changes of the cross sections, which indicate compound states, if the variation of the wavelength of the colliding electrons in this energy range is small compared with the dimensions of the scatterer. This excludes diffraction effects as a reason for the cross section changes. Near the resonance energy, the cross section may increase and/or decrease, depending on the values of two scattering phases. The first is the phase of the outgoing electron wave of the direct collision process with the molecule M

$$M+e \rightarrow Mj^*+e,$$

and the second, the value of the phase of the *one* (spherical for atoms, spheroidal for diatomics) partial wave, which results from the auto-ionization process:

$$M+e \rightarrow M^{*-} \rightarrow Mj^*+e$$

In different channels j the same resonance may look different, since the line shape (interference structure) depends on the direct phase shift and on the scattering angle. Therefore, the analysis of experimentally obtained interference structures allows for a determination of phase shifts[7] for the direct process.

In general, the three methods are complementary to each other. Without going into details, it may be said that the absorption method (i) is a relatively simple experiment, which measures with high accuracy the energy position and possibly the absolute, total cross section of the resonance; whereas the measurement (ii) of the elastic and inelastic differential cross section follows through details of the formation and decomposition (in different reaction channels) of the compound state. It is to be expected that theories (especially those adjusting few parameters) that may well explain the results of (i) may completely fail to explain the results of (ii). The measurement of the negative (stable) ion which is formed in the dissociative attachment process

$$AB+e \rightarrow AB^{*-} \rightarrow A+B^-$$

strongly indicates the existence of the short-lived molecular negative ion state, even if the resonance cannot be detected as a sharp structure in the electron scattering.[11,12] Such a situation exists for electron collisions with H_2 in the energy range from zero to about 8 eV. Here Schulz[5] and Menendez and Holt[13] have shown that H_2 molecules are vibrationally (v = 1 and 2) excited after the electron collision, and Schulz and Asundi[10] detected H^- ions above 3.75 - eV collision energy. In the present work it is shown that a combined measurement of the energy and angular dependence of (e - H_2) scattering also reveals a structureless resonance and in addition is able to yield the configuration of the compound state as well as differential elastic and inelastic cross sections, which

are useful for a thorough comparison with theory.

To accomplish this, it is necessary to use an electron-optical system whose transmission is independent of the energy of the electrons before and after the collisions. Such a system is described in the next paragraph. In the last section of this paper we give results for the energy and angular distributions of scattered electrons from CO and H_2, and compare these results with similar data on the resonance scattering of low-energy electrons by N_2.

APPARATUS

A diagram of the apparatus is shown in Fig. 1 and is referred to in the following description: The apparatus has been partly described in earlier papers.[7,8,14] For the energy selection of the primary electron beam, a 127° electrostatic selector is used. The full-width of the beam at half maximum is 50 meV and for energies greater than 0.3 eV a beam current of approximately 5×10^{-8} A is obtained. The actual selector angle is only 119° in order to compensate for fringing field effects. These effects are determined mainly by the distance (1 mm) of electrodes 2 and 3 (or 10 and 11) from the cylindrical deflector grids (of potential V_1 and V_2, respectively) and by their potential, which is $(V_1+V_2)/2$. The scattering center is defined by the intersection of the electron beam and a gas beam (pressure 10^{-3} Torr). The scattered electrons are energy analyzed in the analyzer system, which has the same dimensions as the selector system. The analyzer can be rotated from 0 to 110° with respect to the incident beam.

Electrons which have passed through the analyzer system are detected by a multiplier whose output pulses (10^{-7} sec duration, 20 mV average height) are amplified, discriminated from dark pulses (<3 mV), shaped (1×10^{-6} sec duration, 20 V peak height) and fed into one of the detection systems. The count rates depend on the reaction cross section and the scattering angle.

For low count rates (20 cps) the multichannel analyzer is used continuously for up to eight hours. The channel number into which counts are stored is proportional to the electron impact energy. Large count rates are integrated by the count-rate meter. For cases in which the signal is masked by a large background count rate, the gas beam is intensity modulated and the lock-in circuit or the multichannel analyzer is used. All three detection systems are connected to an X-Y recorder whose Y axis records the signal intensity corresponding to the X-axis value of the energy loss or impact energy. The angular resolution is better than ± 2°.

The cathode system has been changed with respect to the arrangement used earlier. It contains a thoriated tungsten hairpin cathode, which is essentially a point source for the electrons with practically no potential drop across the effective emission region. The energy half-width of the emitted electrons is about 0.4 eV. The dc current through the filament is 2 A. The magnetic field arising from this current is small because of the geometry of the filament. The reflector and electrode 1 form an immersion lens with a focus at electrode 2. Electrodes 1a and 1b serve as two pairs of perpendicular deflector plates to be used for correcting any misalignment in the beam. The whole system forms an electron beam of 1-eV energy, 10^{-6} A, and rather low angular divergence. This beam is injected into the selector.

The selector grids are made from woven mesh of 90% transmission. It is elastic enough to survive bake-out temperatures of 400°C without permanent deformation. Outside the mesh are solid plates (plus 10 V with respect to V_1 and V_2), which are covered with porous gold black in order to retain stray electrons, i.e., to decrease the space charge in the center of the selector.

The lens system L_4, L_5 accelerates the electrons to the proper energy and guarantees a focus at the scattering center. Electrode 6 is at ground potential. L_4 and L_5 are split into two halves perpendicular and parallel, respectively, to the plane of the figure. They are also used as deflector plates for alignment of the electron beam. To ensure a transmission which is practically independent of the energy of the electrons, the lens potentials V_{L4} and V_{L5} (and V_{L8} and V_{L9}) are automatically changed with the acceleration voltage V_E between electrodes 3 and 6 as

$$V_{L_K} = V_{OL_K} + C_{L_K} V_E, \quad K = 4, 5,$$

where V_{OL4} and V_{OL5} are constant potentials and C_{L4} and C_{L5} are constant factors. This type of variation seems necessary, since the electrons enter the immersion lens system with about 1 eV kinetic energy and after acceleration (or deceleration) have energies of from 0.3 to 30 eV or more.

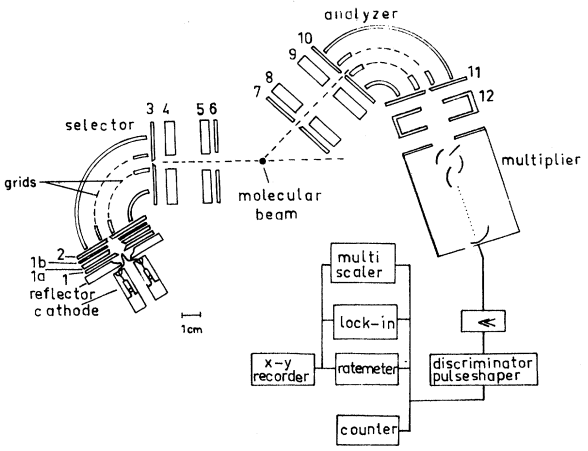

FIG. 1: Schematic drawing of the experimental arrangement. The selector system produces an electron beam of about 5×10^{-8} A at energies larger than 0.3 eV. The analyzer system can be rotated in the angular range from 0° to 110°. The over-all energy resolution of the system is 0.05 eV. The count rates range from 20 cps to a maximum of 5×10^4 cps.

The adjustment is done just by setting V_E to provide the minimum desired electron kinetic energy after acceleration. V_{OL4} and V_{OL5} are then adjusted so that the beam is focused at the scattering center. Next, V_E is set to provide the maximum desired electron kinetic energy after acceleration and C_{L4} and C_{L5} are adjusted to refocus the beam at the scattering center. In the same way, the potentials of the deflector plates are chosen. As a test for the transmission, the energy dependence of the elastic differential cross section of helium (or any other well-known cross section) is measured. After this procedure (occasionally it has to be done iteratively), the transmission is constant within a few percent over an energy range from E_{min} to E_{max} with E_{max}/E_{min} ~ 10 to 20. Our intensity values are correct within about 5%.

The molecular beam is formed by a tube 10 mm long and 1 mm in diameter. The beam broadens rapidly beyond the end of this tube. The electron beam intersects the neutral beam about 2 mm from the tube end. The gas pressure at this point is between 10^{-3} to max 10^{-2} Torr. With the beam on, the gas pressure in the vacuum chamber increases from 10^{-7} to 10^{-5} Torr.

All electrodes of the selector, analyzer, and lenses are made from demagnetized stainless steel, gold plated and baked to 400°C. During operation the whole system is at room temperature, except for the injection system of the selector, which is at about 100°C. Every two weeks the entire system is baked for several hours. This procedure ensures stable conditions, so that measurements over many hours can be made without readadjustments.

The magentic field near the scattering center is compensated to within 2 mG and the remaining stray electric field is less than about 5 mV. For the measurement of energy-loss spectra (for example, Fig. 3) the primary energy Ep is fixed and the deceleration voltage V_E of the lens system of the analyzer is varied; for excitation functions of an inelastic channel (see Figs. 4 and 7), only electrons which have lost a fixed energy ΔE pass through the analyzer. In this case Ep and the analyzer potential Va are varied, so that $Ep = \nabla E + |e|Va$.

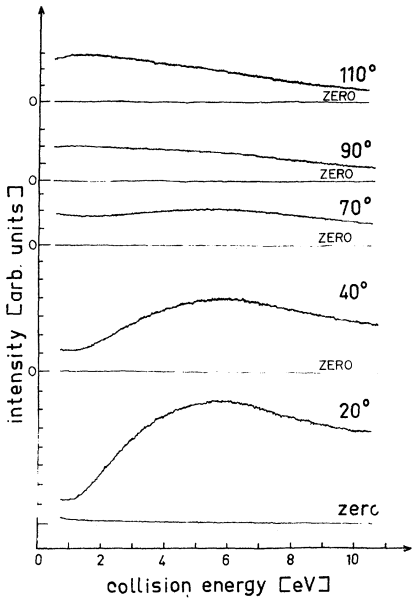

FIG. 2: Elastic scattering of electrons from H_2. The curves show the scattered intensity (differential cross section) as a function of the energy of the colliding electrons for different values of the scattering angle. *The intensity scale for all curves is the same.* The zero lines represent the gas-off condition, the remaining count rate is then only a few percent of the signal (gas on).

EXPERIMENTAL RESULTS

1. $e - H_2$

Results for the elastic scattering of low-energy monochromatic electrons from H_2, i.e., the energy dependence for several scattering angles, are given in Fig. 2. Although by now the appearance of an H_2^- resonant state in this region is well documented, [5,10,12,15,16,17] the absences of peaked structure in the various channels and the evident short lifetime of this state[10,12,15,16,17] put in question the usefulness of the resonant model in describing this state of H_2^-. In fact, in the total scattering measurements of Ref. 11, the lack of peaked structure was given as evidence of the absence of a resonance in this energy range. Evidence for a resonance mechanism is indicated by Fig. 3.[10] Figure 3 shows the energy loss spectrum of the electrons after the excitation collision, i.e., the relative transition probabilities for the excitation of 0, 1, 2, 3, and 4 vibrational quanta in H_2. By momentum transfer arguments, it can be shown that, vibrational excitation can only occur to the significant extent that it does if the electronic configuration of the molecule changes, which, in this energy range, is only possible via a negative ion state. Moreover, since the probability ratios for the transitions into $v = 0, 1, 2, 3$, for Ep = 4 eV, are 3400 : 120 : 10 : 1 (Fig. 3), it is plausible that the resonance process gives a large contribution to the elastic cross section. For the transition into $v = 1$ and $v = 2$, a value of the ratio has already been determined by Schulz[5] (7 : 1) and by Menendez and Holt (10 : 1). This ratio depends of course on the energy Ep (see also Fig. 5). The large decrease of the transition probability for the excitation of higher vibrational quantum numbers at all primary energies could possibly indicate that the equilibrium distance between the two protons in H_2 and H_2^- is not greatly different.

A complete analysis of the differential elastic scattering, i.e., a partition into the potential and resonance scattering, is not possible from the experimental data without making assumptions concerning the phase shifts of the potential collision cross section. With increasing primary energy, the number of partial waves significantly contributing to potential scattering also increases. These waves interfere with the resonance wave and with each other. This can be seen quali-

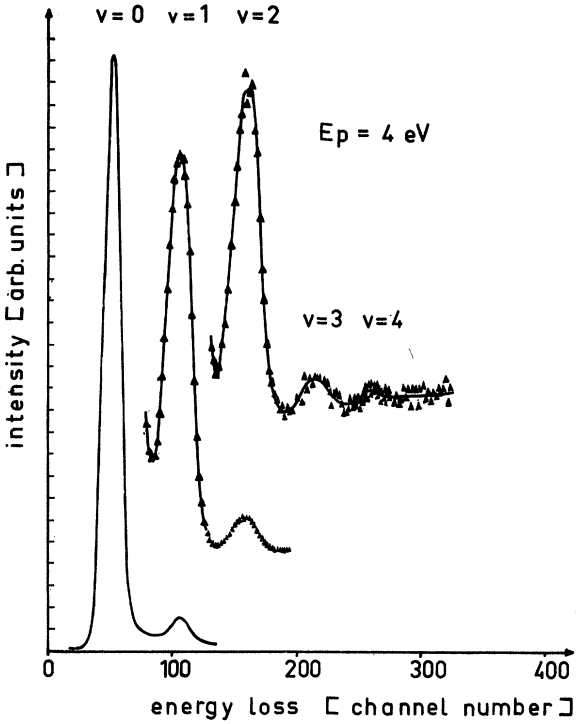

FIG. 3: Energy loss spectrum of 4 eV electrons after collision with H_2 molecules. The energy resolution for this measurement is decreased in order to increase the sensitivity. $v=0$ represents the elastic scattering; and $v=1$, 2, 3, and 4 represent the excitation of v vibrational quanta of the neutral molecule via the short-lived negative ion state $^2\Sigma_u^+$. *The ratios of the peaks are discussed in the text.* The count rate at the peak of $v=1$ is 3×10^5 counts/sec, the time of measurement 4 hours.

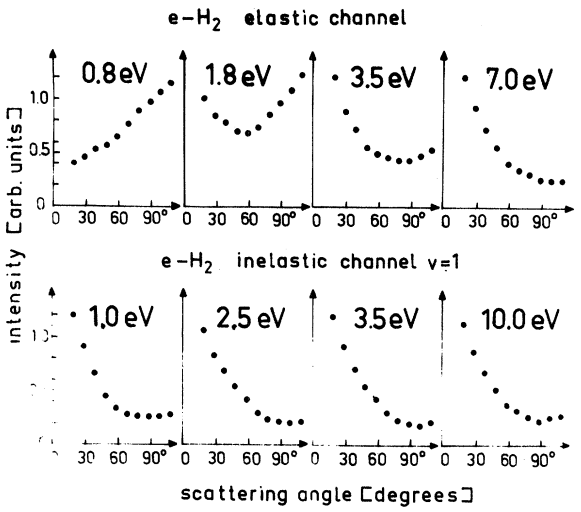

FIG. 4: Angular dependences of the elastically and inelastically (excitation of one vibrational quantum) scattered electrons from H_2 for different collision energies. The change of the angular dependence with energy in the elastic channel is due to the interference of several partial waves, whose phase shifts change with energy. This is typical for any potential scattering. In contrast, the constancy of the curve shapes for the inelastic channel shows that only one partial wave results from the auto-ionization of the negative-ion state of H_2. The shape of the angular dependence leads to the experimental confirmation of the configuration $^2\Sigma_u^+$ of the H_2^-.

tatively from the angular dependences of the elastic cross section, which change markedly with the energy of the colliding electrons (Fig. 4).

Angular distributions for the inelastic channels $v=1$ and $v=2$ (examples are given in the lower part of Fig. 4) have been taken for fixed values of the collision energy ranging from 0.75 eV up to 10 eV. All these curves are identical to within experimental error (approximately 10% for each point). This shows, without any need for a numerical analysis of p-wave data, that the excitation of a vibrational quantum at all energies (including $v=1$ near threshold) occurs via a resonant H_2^- state. This state clearly has a well-defined set of quantum numbers. For a nonresonant or direct excitation, the angular dependence is expected and is known to change with incoming electron energy. From the shape of the angular dependence for the inelastic channels it can be stated that the compound state must have *ungerade* symmetry, because the p-wave part dominates. A p wave corresponds to an *ungerade* eigenfunction. The configuration of the relevant H_2^- resonance state has been predicted to be $^2\Sigma_u^+$ by Bardsley *et al.*,[15] and Taylor, *et al.*[12] This prediction is in qualitative agreement with the measured angular distribution. The given configuration implies that the incoming electron is trapped into a $p\sigma$ orbital and therefore the auto-ionized electron will show a predominant p-wave dependence (see the more detailed discussion below).

Results on the excitation function for the excitation of $v=1,2$ and 3 are given in Fig. 5. The recorder traces are taken at a scattering angle of 20°. The additional points imposed on the recorder traced in Fig. 5 represent partly data from other angles and partly values deduced from energy loss spectra. Figure 5 shows that the shapes of the excitation functions do not change with angle. This is identical with the result that the angular dependences are independent of the collision energy. The absolute values of the cross sections have been obtained by integration over the angular distributions and normalization to the known absolute total elastic cross section. The ratios of the elastic and inelastic cross sections were obtained separately by energy loss spectra as shown in Fig. 3.

Schulz and Asundi[10] have measured the cross section for dissociative attachment which can occur above 3.75 eV. This is a very direct method to determine unambiguously the existence of a resonance state of very short lifetime in molecules, even if they do not show sharp resonance structures. These authors were also able to de-

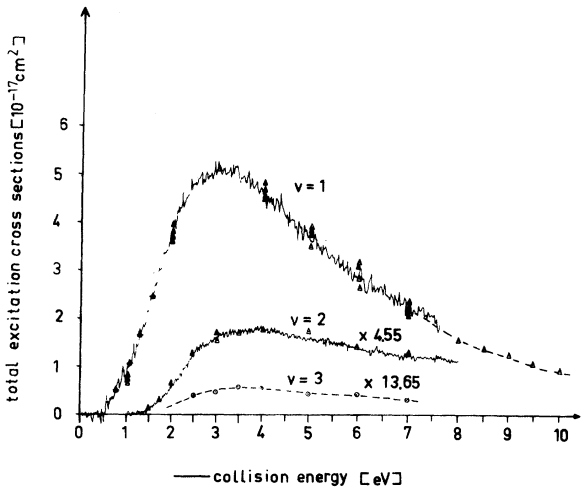

FIG. 5: Energy dependences of the total cross sections for the excitation of 1, 2, and 3 vibrational states by electron collision with H_2. The curves $v=2$ and $v=3$ are enlarged by a factors of 4.55 and 13.65, respectively. with respect to the ordinate scale. △ and + refer to additional measurements taken from energy loss spectra and at various scattering angles.

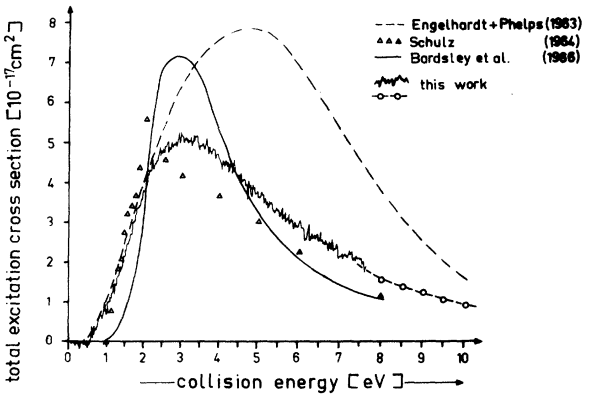

FIG. 6: Comparison of the total cross sections for the excitation of one vibrational quantum of H_2 by electron impact. Engelhardt and Phelps derived their curve from a swarm experiment, Schulz measured the electron scattering at 72°, the present authors measured electron scattering in the range 20°-110°; the full line curve is taken from a theoretical paper of Bardsley *et al*. Menendez and Holt (not shown) published the excitation cross section in arbitrary units in the energy range from 0.54 to 1.4 eV, in agreement with Engelhardt *et al*. and the present work.

duce the half-width of this state to be approximately 3 eV. This value is in good agreement with theoretical predictions.

It is not possible without assumptions to extract from our measurements a good value for the half-width of the resonance state. The excitation function $v=1$ of Fig. 5 can in principle be composed of resonance contributions for the excitation of different vibrational states v' of the H_2^- state, and we do not know and cannot see from the experiment how effective these excitations are. But limits for the half-width can be deduced from the excitation functions of Fig. 5. The shapes of these curves are determined by a number of factors. First there is a flux-factor k/k_0, which tends to emphasize the increasing nature of the inelastic cross section near threshold compared to its "natural" shape. Second, if only one vibrational state ($v'=0$) of the H_2^- ion would be involved in the cross section of the excitation functions of Fig. 4, its shape would be of Breit-Wigner form, i.e., symmetric about its maximum and the half-width could be measured directly.

But, since the excitation functions have a high-energy tail, which falls off slowly, several vibrational states $v'>0$ and numerous unbound nuclear motion states must be involved in the process. Taking these arguments into account, the half-width cannot be larger than 4 eV and should not be smaller than 2 eV.

The maximum of the excitation function $v=1$ is at 3 eV. Therefore, the energy positions of maximum of the overlapping vibrational states $v'=0$, $v'=1$ ($v'>2$?) of the H_2^- ion should be near this energy. The actual position of the $v'=0$ states of H_2^- ion should be at somewhat lower energy. This is not in agreement with calculations of Ref. 15, but does generally agree with rough estimates of these levels in Ref. 16. Figure 6 shows the absolute inelastic cross section $v=1$ for electron collision with H_2 in the energy range from 0 to 10 eV. It is compared with measurements of Schulz[5] and Engelhard and Phelps[19] (swarm experiment). Schulz obtained his curve also from the measurement of the inelastically scattered electrons, but he used the assumption that the angular dependence of the scattered electrons is isotropic. Near 3-eV collision energy, all experimental determinations are in rather good agreement, whereas the swarm experiment gives too high values for higher energies and Schulz's measurements disagree near threshold. That the $v=1$ excitation starts at threshold (0.54 eV), was also found by Menendez and Holt[13] (relative intensities). The general curve shape (except near threshold) and the position of the maximum of the partly calculated, partly fitted curve of Bardsley *et al.*[17] is, in spite of the fact that their potential curve gives no vibrational bound states, in good agreement with our experimental result.

Above 8-eV collision energy one expects the formation of another short-lived nonbonding negative ion state ($^2\Sigma_g^+$) of the hydrogen molecule. This state has *gerade* symmetry and therefore a different behavior of the angular distribution of the ejected electrons. Within experimental error we cannot detect any changes, whether in the cross sections or of the angular distribution (see also Fig. 4). In spite of our failure in these experiments to see this state (it is detected in dissociative attachment experiments), we expect the angular distribution method to be (in channels where elastic scattering tends to drop out) a way of looking for nonbonded

resonant states. These states would not show peak structure even if they were long lived because of the absence of discrete levels of nuclear motion. On the other hand they would have characteristic, symmetry-determined angular dependences that remain fixed over various energy ranges and in various channels.

2. e-CO

In Fig. 7 is shown the energy dependence of the elastic scattering of electrons with CO for several scattering angles. The angular dependence for several fixed values of the collision energy is given in Fig. 9. Potential scattering dominates the elastic cross section below 1 eV and for energies higher than 4 eV. At energies between 1 and 4 eV the resonance process is dominant (see also Fig. 7). From all curves the energy position of the vibrational ground state of the CO^- ion is determined to be 1.5 eV. This $v' = 0$ resonance is only indicated as a shoulder, whereas the higher vibrational states $v' = 1$, 2, 3, and 4 show more structure. The energy difference between the positions of $v' = 0$, 1, ... is about 230, 220, 210, 200 meV, which is somewhat smaller than the corresponding vibrational quantum of the molecular ground state

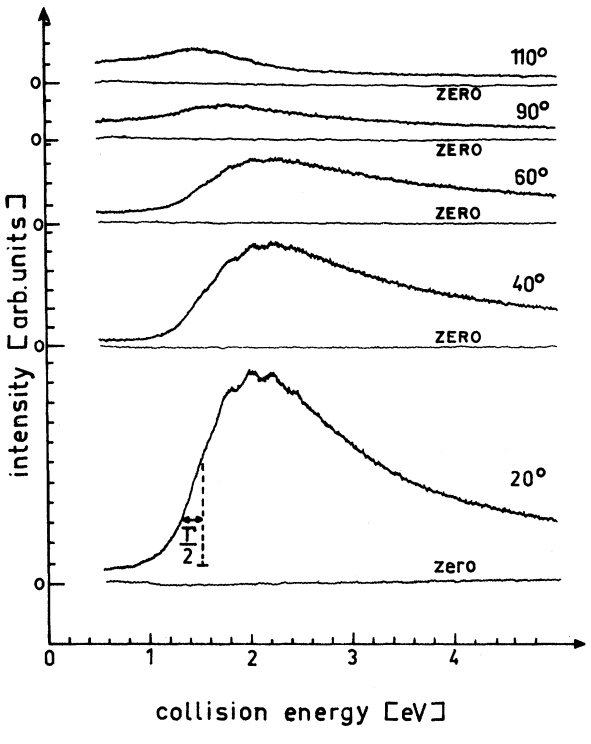

FIG. 7: Energy dependence of elastic differential cross sections for collisions of electrons with CO molecules at different scattering angles. The first resonance peak is only weakly indicated as a shoulder at 1.5 eV. $\Gamma/2$ is an approximate measure for the half-width Γ (full-width at half height, 0.4 eV) of the resonance state. This first peak is better developed in the inelastic scattering (see Fig. 8). The intensity scale for all curves is the same.

(270, ... meV). This behavior is similar to the case of N_2,[7,8] where the vibrational spacings of N_2^- are smaller than the corresponding ones in N_2. This result is consistent with the single-particle model[12], in which one pictures these low-energy resonances as an electron orbiting the ground-state configuration. Since the first empty orbitals of the target are (in all cases here studied) antibonding, the depth of the well of the potential curve is expected to be shallower than that of the target. Accordingly, the vibration levels of the resonance species should be more closely spaced than those of the target.

The half-width Γ (full-width at half height) of the resonance state CO^- is approximately 400 meV. This value has been determined from $\Gamma/2$ of the resonance $v' = 0$ of the elastic cross section shown in Fig. 7 and the inelastic case of Fig. 8. In both cases the contributions of the direct scattering has been taken into account by linear extrapolation of its values below 1 eV.

The maximum of the resonance cross section apparently occurs close to 2 eV for the transition CO $(v = 0) - CO^-$ $(v' = 1, 2)$. This indicates that the equilibrium distance of the nuclei in CO^- is somewhat larger than in CO. This again fits the single-particle picture in which a nonbonding orbital is occupied. The resonance state internuclear distance is estimated to be 1.17 Å, while for CO, it is 1.13 Å. The angular dependences of the elastic scattering is the result of the interference between the resonance wave and the waves of the potential scattering as well as the interference between different waves of the potential scattering. This is demonstrated in Fig. 9 (upper row) by the rapid change of the angular dependence with collision energy.

Figure 8 shows our results of the energy dependence of the vibrational excitation $v = 1$, 2, ..., 7 of the CO molecule in its electronic ground state. This measurement has been made at a detection angle of 20°. These results are in full agreement with all details of the measurements of the same kind, which had been published by Schulz[5] in 1964. His measurements had been taken at 72°. The curve shapes, i.e., the ratios of intensities for different collision energies within a curve with one v value as well as with different v values, do not change with angle (see Fig. 9) in the range from 10° to 110°, which indicates that the Born-Oppenheimer approximation should be valid for the electron attachment and the autoionization process. Following the Aufbau principle and the single-particle model, the attached electron should be trapped in a $p\pi$ orbital leading to a $^2\Pi$ state for the CO^-. This configuration is in qualitative agreement with the experimental angular dependence of the detached electrons.

From his measurements, Schulz[5] has determined the total, absolute cross section for the inelastic scattering by summing over all intensities for the vibrational excitation of $v = 1$ up to $v = 8$ as a function of collision energy. The integration over the scattering angles he replaced by the assumption that the angular distribution of the resonance scattering is isotropic. Taking into account the observed angular dependence (see Fig. 9) in the same way

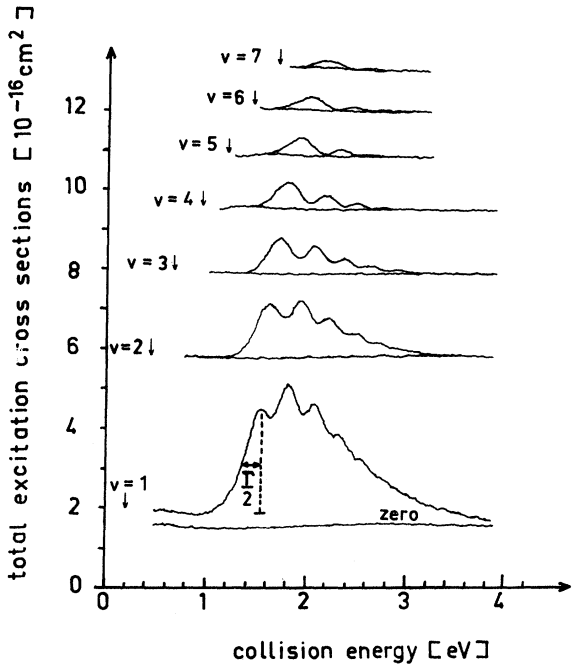

FIG. 8: Absolute total cross sections for the excitation of CO molecules into the vth vibrational state as a function of the energy of the colliding electrons. The arrows indicate the threshold energies for the excitations (for $\Gamma/2$ see Fig. 7).

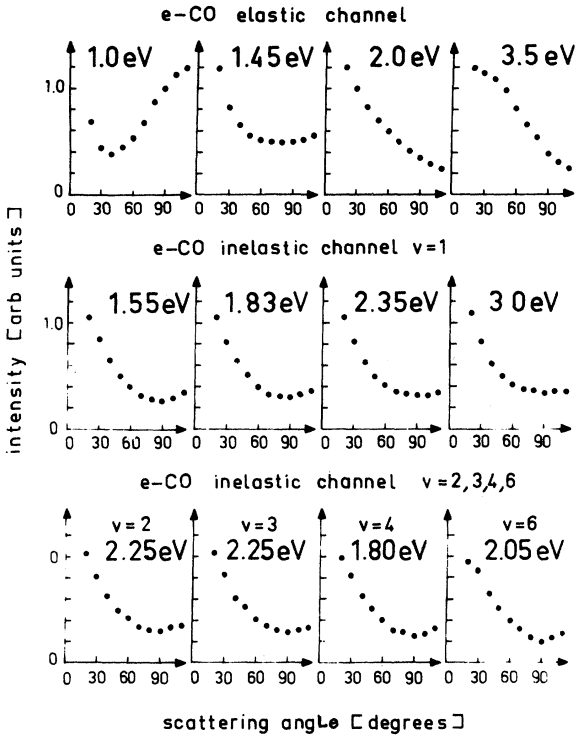

FIG. 9: Angular dependences of the elastic and inelastic scattering of electrons by CO molecules at different collision energies. In the elastic channel (upper row), the angular dependence changes rapidly with energy since the scattering contains several partial waves with varying phase shifts (energy close to threshold). The constancy of the curve shapes for all inelastic channels and energies within the resonance region demonstrates that a compound state with a well-defined set of quantum numbers auto-ionizes and therefore only one outgoing partial wave can be detected.

as described for the case of H_2 we get a value of 3.5×10^{-16} cm^2 excitation (Fig. 8).

The intensity of the excitation function $v=1$ does not drop to zero below 1 eV in contrast to the excitation functions for $v \geq 2$. This means that one vibrational quantum of the CO molecule can be excited by the collision of the molecule with a slow electron via a nonresonant process. The figure also shows that the cross section for this direct excitation process decreases with increasing collision energy, i.e., above 4 eV the scattered intensity in the $v=1$ channel is markedly smaller than for energies below 1 eV. Within experimental error, N_2 does not show this direct excitation below the resonance energy (see Fig. 10). This conclusion is in excellent agreement with the results of Phelp's swarm experiments.[20] This latter experiment has the advantage of being able to measure threshold behavior more accurately than the techniques of this paper.[20] For N_2, it is found[20] that Chen's[21] resonant scattering formulas fit the swarm data at threshold. For CO, Chen's resonant scattering formulas did not fit the data at threshold. He therefore concludes that *at threshold* N_2, vibrational excitation is dominated by a resonant process, while for CO the process of excitation is potential scattering dominated. This of course emphasizes the importance of the effect of the permanent dipole in increasing lower energy direct inelastic scattering cross sections.

The apparent shift of the energy position of the first peak for increasing quantum number v and the broadening of this first peak appears experimentally similar as in N_2. Since N_2 and CO and N_2^- and CO^- are, respectively, iso-electronic, one expects this similar behavior. This has already been discussed by Schulz.[5] The explanation of this effect has been given by Chen [20] and Herzenberg and Mandl.[22] The transition probabilities to the different final channel v of the molecule contain the product of the Franck-Condon factors $\langle v=0|v'\rangle$ for the excitation of the compound state v' and $\langle v'|v\rangle$ for the autoionization into state v of the molecule. The energy position of the resonances v' remain unchanged, but the cross section σ $(0 \rightarrow v)$ decreases with increasing v. Figure 8 shows that for $v=4$ or 5 the first peak has disappeared. For the case of N_2 this apparent energy shift of the first peak (and also the others) as a consequence of the decrease of the Franck-Condon factors can be seen in the experiment much more nicely than for CO, since the half-width of the N_2^- resonance peaks is somewhat larger (~250 meV) than in CO.

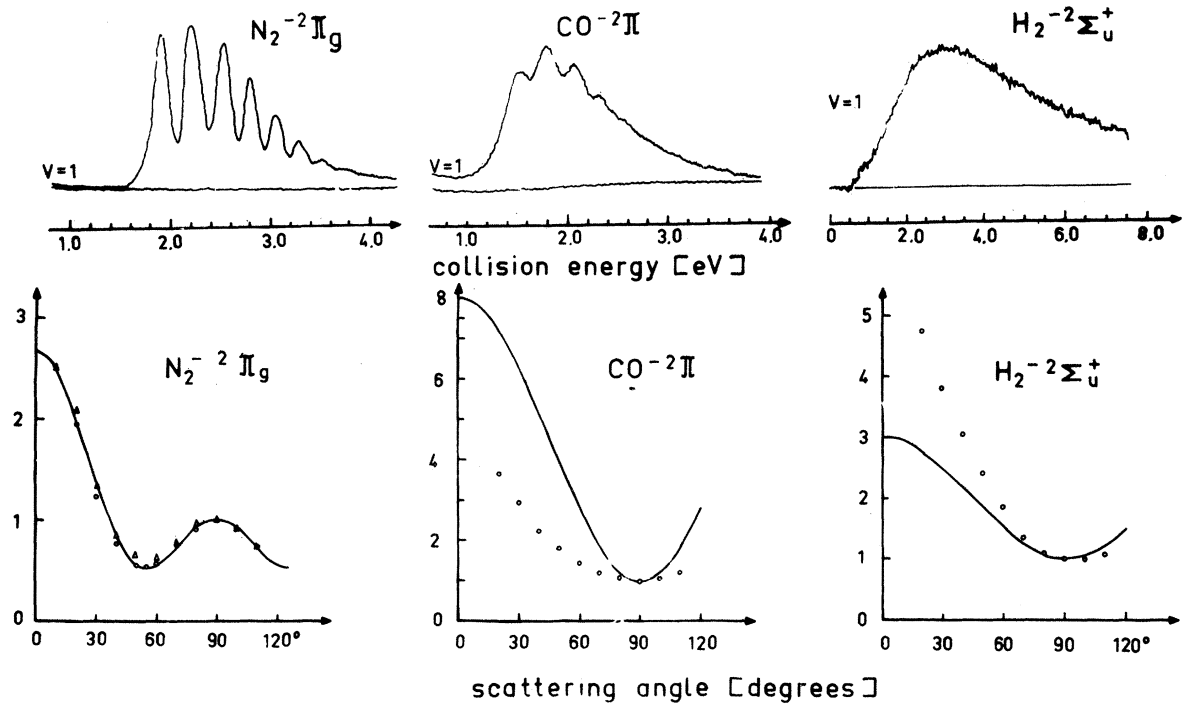

FIG. 10: Comparison of the energy dependences (upper row) and the angular dependences (below) of the resonant excitation of one vibrational quantum of N_2, CO, and H_2. The full lines in the graphs of the angular dependences represent the simplest theoretical expressions (Ref. 26) for the auto-ionization for the trapped electron. These expressions are

H_2 $p\sigma$	$\sigma(\theta) \alpha 1+2\cos^2\theta$.
CO $p\pi$	$\sigma(\theta) \alpha 1+7\cos^2\theta$.
N_2 $d\pi$	$\sigma(\theta) \alpha 1-3\cos^2\theta+\frac{14}{3}\cos^4\theta$.

They are normalized, together with the experimental data, to 1 at 90°. It will be shown in Ref. 26 that normalization of the CO form to an angle near zero degrees gives a much better apparent agreement than is evidenced from this figure. The normalization is freely adjustable.

COMPARISON OF THE LOW-ENERGY RESONANCES IN H_2, CO, AND N_2

The short-lived negative ion states of H_2, CO, and N_2 show similarities, but also differences, in their physical behavior (compare Fig. 10). One of the similarities is the energy position of the negative ion potential curve minimum. The energy position of the vibrational state $v'=0$ for H_2^- is smaller than 3 eV, that for CO^- at 1.5 eV and for N_2^- at 1.89 eV. These resonances must be of the type called single particle (see, for discussion, Ref. 12). They depend on (*i*) the symmetry of the target; (*ii*) the lowest energy unoccupied molecular orbitals and their symmetry (especially as coupled to the target); and (*iii*) the permanent and induced moments of the target potential at the average extra electron radius. It is pictured that the extra electron is trapped (in a large, compared to internuclear distance, orbit) by the distorted charge distribution of the target plus an angular momentum barrier. (Note all resonant angular dependences for above threshold resonances are invariably for partial l waves with $l'>0$). The electron does not have a great core penetration probability and hence probes the outer parts of the molecular potential field. In this latter sense it is somewhat analogous to the shape resonances of nuclear physics. Another similarity is the order of magnitude of the half-widths. For the three resonances, it is $\Gamma_{H_2^-} \sim 3$ eV, $\Gamma_{CO^-} \sim 0.40$ eV, and $\Gamma_{N_2^-} \approx 0.150$ eV. These values are as expected to be much larger than the Γ values of Feshback's core excited I resonances,[12] for example, $\Gamma(H^-2^1S) \approx 0.043$ eV,[23] $\Gamma(H^-2^3P) \approx 0.009$ eV,[23] $\Gamma(He^-\ 2^2S) \approx 0.012$ eV,[24] $\Gamma(Ne^-\ 3^2P_{3/2,1/2}) \approx 0.0014$ eV, $\Gamma(Ar^-\ 4^2P_{3/2,1/2}) < 0.001$ eV.[7]

The differences for the detailed values of the half-widths and energy positions can be rationalized, using different potential parameters in a model potential. For large distance r between electron and target particle, the potential is

$$V_{r>} = -\frac{\alpha e^2}{2r^4} + \frac{h^2}{2m}\frac{l(l+1)}{r^2}$$

where α is the polarizability of the molecule and l the angular momentum quantum number of the autoionizing electron. The superposition of the attractive polarization potential with the repulsive centrifugal potential results in a large wavelength (around 10 Å) for the electron, so that it can tunnel through this wall and can be trapped for some

time. For the case of N_2 and CO the polarizability α is about equal, but for N_2, $l=2$ and for CO, $l=1$. This means that for N_2 the potential wall is larger and broader at the relevant energies. Therefore, one might expect the $N_2(d\pi g, {}^2\Pi g)$ resonance energy to be higher and the lifetime larger than the values for the CO^- $(p\pi, {}^2\Pi)$ resonance. For H_2 the polarizability is smaller than for N_2 and CO and $l=1$. In this model the H_2^- $(p\sigma, {}^2\Sigma_u^+)$ state should have a larger half-width than the N_2^- and CO^- resonances. A detailed description of the influences of the values of the potential parameters on the N_2^- and CO^- resonance has been given by Bradsley, Mandl and Wood.[25]

The single-particle model, so far described, lends itself in these cases to easy qualitative prediction of the resonant angular dependence in the inelastic channel where, by momentum transfer arguments, the potential scattering is diminished. Since the target electronic wave functions are Σ_g or Σ in all cases here considered, one can envision them to be predominantly S wave in a one-center expansion. The angular dependence then depends on the symmetry of the newly occupied orbit; σ_u, π_g, and π for H_2, N_2 and CO, respectively. Because of its large radius, this new orbit can be expanded in a one-center expansion and the first term allowed by the conservation of orbital angular momentum along the internuclear axis, and by conservation of parity is retained. This gives the l wave responsible for the scattering. It leads to a prediction of a "d" or $d\Pi$ wave for N_2^-, ${}^2\Delta g$ and "p" wave for CO^- ${}^2\Pi$ and H_2^- ${}^2\Sigma^+$ over the total energy range of the resonance and in all final vibrational channels. The predictions must be averaged over the orientation of the molecule relative to the incident direction. The resulting ideal angular dependences are given in the caption of Fig. 10 and plotted in Fig. 10. A glance at Fig. 4 to 10 show that qualitatively the d and p predictions hold, as do those of energy and channel (inelastic) independence. In fact, from Fig. 10 for N_2, quantitative agreement is achieved. For CO and H_2, the situation is not as simple. To completely analyze the reasons that cause perfect agreement to be lost requires a more complete listing of the mathematical assumptions made in going from a rigorous theory to these simple predictions. This will all be done in a future paper[26] where it is also shown that renormalization of the theoretical angular dependence leads to near quantitative agreement for CO also.

We acknowledge the financial support of the Deutsche Forschungsgemeinschaft and would like to thank Dr. F. Mandl for many helpful discussions. H. S. T. was partially supported by a National Science Foundation Grant, Contract No. GP-4284, and the Research Corporation. H. S. T. would like to thank J. K. Rice of the California Institute of Technology for aid with this manuscript.

---

*Now at the Department of Chemistry, University of Southern California, Los Angeles, California.

†Alfred P. Sloan Foundation Fellow.

[1]C. E. Kuyatt, S. R. Mielczarek, and J. Arol Simpson, Phys. Rev. Letters 12, 293 (1964).

[2]D. E. Golden and H. W. Bandel, Phys. Rev. Letters 14, 1010 (1965).

[3]M. J. W. Boness and J. B. Hasted, Phys. Letters 21, 526 (1966).

[4]G. J. Schulz, Phys. Rev. 125, 229 (1962).

[5]G. J. Schulz, Phys. Rev. 135, A988 (1964).

[6]H. G. M. Heidemann, C. E. Kuyatt, and G. E. Chamberlain, J. Chem. Phys. 43, 355 (1966).

[7]D. Andrick and H. Ehrhardt, Z. Physik 192, 99 (1966).

[8]H. Ehrhardt and K. Willmann, Z. Physik 204, 462 (1967).

[9]D. Rapp, T. E. Sharp, and D. D. Briglia, Phys. Rev. Letters 14, 533 (1965).

[10]G. J. Schultz and R. K. Asundi, Phys. Rev. 158, 25 (1967).

[11]D. E. Golden and H. Nakano, Phys. Rev. 144, 71 (1966).

[12]H. Taylor, G. Nazeroff, and A. Golebiewski, J. Chem. Phys. 18, 353 (1967).

[13]M. G. Menendez and H. K. Holt, J. Chem. Phys. 45, 2743 (1966).

[14]H. Ehrhardt and K. Willman, Z. Physik 203, 1 (1967).

[15]J. N. Bardsley, A. Herzenberg, and F. Mandl, Proc. Phys. Soc. (London) 89, 305 (1966).

[16]H. Taylor, I. Eliezer, and J. K. Williams, J. Chem. Phys. 47, 2165 (1967).

[17]J. N. Bardsley, A. Herzenberg, and F. Mandl, Proc. Phys. Soc. (London) 89, 321 (1966).

[18]In Fig. 3 the energy resolution of the apparatus has been decreased to about 150-200 meV in order to obtain a higher sensitivity.

[19]A. G. Engelhardt and A. V. Phelps, Phys. Rev. 131, 2115 (1963).

[20]A. V. Phelps, Rev. Mod. Phys. 40, 399 (1968).

[21]J. C. Y. Chen, J. Chem. Phys. 45, 2710 (1966).

[22]A. Herzenberg and F. Mandl, Proc. Roy. Soc. (London) A270, 48 (1962).

[23]J. W. McGowan, Phys. Rev. 156, 165 (1967).

[24]D. Andrick and H. Ehrhardt, unpublished.

[25]J. N. Bardsley, F. Mandl, and A. R. Wood, Chem. Phys. Letters 1, 359 (1967).

[26]T. F. O'Malley and H. S. Taylor, to be published.